

## **Suppression of reactive oxygen species generation in heart mitochondria from anoxic turtles: the role of complex I S-nitrosation**

Amanda Bundgaard<sup>1</sup>, Andrew M. James<sup>2</sup>, William Joyce<sup>1</sup>, Michael P. Murphy<sup>2</sup> & Angela Fago<sup>1\*</sup>

<sup>1</sup>Department of Biosciences, Aarhus University, DK-8000 Aarhus C, Denmark

<sup>2</sup>MRC Mitochondrial Biology Unit, University of Cambridge, CB2 0XY Cambridge, United Kingdom

\*corresponding author (angela.fago@bios.au.dk)

**Keywords:** anoxia – respiration – complex I – S-nitrosation – mitochondria – reactive oxygen species

**Summary statement:** Heart mitochondria show suppressed reactive oxygen species (ROS) generation when isolated from anoxic turtles. Surprisingly, complex I S-nitrosation, a potent modification inhibiting ROS production, is not involved in this response.

**Acknowledgements:** We thank Hans Gesser for his help with the experimental design and Per Guldhammer Henriksen for assisting with turtle acclimation.

**Competing interests:** MPM holds a patent on technology described in this manuscript. No other competing interests.

**Funding:** This work was funded by a grant from the Danish Council for Independent Research, Natural Sciences (grant 4181-00094 to AF), the Medical Research Council UK (grant MC\_U105663142 to MPM) and a Wellcome Trust Investigator award (grant 110159/Z/15/Z to MPM).

## List of abbreviations

**BN-PAGE:** Blue Native polyacrylamide gel electrophoresis - **BSA:** Bovine serum albumin - **DDM:** Dodecyl maltoside - **DTNB:** 5,5-Dithiobis(2-nitrobenzoic acid) - **DTPA:** Diethylenetriaminepentaacetic acid - **DTT:** Dithiothreitol - **EDTA:** Ethylenediaminetetraacetic acid - **EGTA:** ethylene glycol-bis( $\beta$ -aminoethyl ether)-N,N,N',N'-tetraacetic acid - **FCCP:** Carbonyl cyanide-p-tri-fluoro-methoxyphenylhydrazone - **GAPDH:** Glyceraldehyde 3-phosphate dehydrogenase - **KCN:** Potassium cyanide - **NADH:** Nicotinamide adenine dinucleotide - **NEM:** N-ethylmaleimide - **PBS:** phosphate-buffered saline - **RET:** Reverse electron transfer - **ROS:** Reactive oxygen species - **TTC:** Triphenyl-tetrazolium chloride

## Abstract

Freshwater turtles (*Trachemys scripta*) are among the very few vertebrates capable of tolerating severe hypoxia and reoxygenation without suffering from damage to the heart. As myocardial ischemia and reperfusion causes a burst of mitochondrial reactive oxygen species (ROS) in mammals, the question arises as to whether, and if so how, this ROS burst is prevented in the turtle heart. We find here that heart mitochondria isolated from turtles acclimated to anoxia produce less ROS than mitochondria from normoxic turtles when consuming succinate. As succinate accumulates in the hypoxic heart and is oxidised when oxygen returns this suggest an adaptation to lessen ROS production. Specific S-nitrosation of complex I can lower ROS in mammals and here we show that turtle complex I activity and ROS production can also be strongly depressed *in vitro* by S-nitrosation. While we can detect *in vivo* endogenous S-nitrosated complex I in turtle heart mitochondria, these levels are unaffected upon anoxia acclimation. Thus while heart mitochondria from anoxia-acclimated turtles generate less ROS and have a lower aerobic capacity than those from normoxic turtles, this is not due to decreases in complex I activity or expression levels. Interestingly, in-gel activity staining reveals that most complex I of heart mitochondria from normoxic and anoxic turtles forms stable supercomplexes with other respiratory enzymes and, in contrast to mammals, these are not disrupted by dodecyl maltoside. Taken together, these results show that, although S-nitrosation of complex I is a potent mechanism to prevent ROS formation upon reoxygenation after anoxia *in vitro*, this is not a major cause of the suppression of ROS production by anoxic turtle heart mitochondria.

## Introduction

Depriving the heart of oxygen for prolonged periods, as may occur during ischemia or whole body hypoxia, can cause profound tissue damage. This is exacerbated upon subsequent reperfusion or reoxygenation because a surge of mitochondrial reactive oxygen species (ROS) is produced that may oxidize proteins, lipids and DNA (Kowaltowski et al., 2009; Murphy and Steenbergen, 2008; Yellon and Hausenloy, 2007). Very few vertebrates are adapted to survive prolonged anoxia and reoxygenation, and in those that are, an important part of this adaptation is avoiding tissue oxidative damage upon reoxygenation (Bickler and Buck, 2007). Among these animals, the extremely anoxia-tolerant freshwater turtles [*Trachemys scripta elegans* (Wied-Neuwied 1839)] survive months of complete anoxia during winter hibernation (Jackson, 2000; Ultsch, 1989; Ultsch and Jackson, 1982) while maintaining overall heart function and ATP levels to sustain circulation for glucose delivery and waste removal (Overgaard et al., 2007; Stecyk et al., 2009; Wasser, 1996). This adaptation to survive prolonged anoxia involves a powerful metabolic suppression (down to ~5% of basal metabolic rate), suppression of *de novo* protein synthesis to save ATP, large glycogen stores in the liver, tolerance of lactate and avoidance of oxidative stress at reoxygenation (Bickler and Buck, 2007; Boutilier and St-Pierre, 2000; Hochachka et al., 1996). Compared to other anoxia tolerant species such as crucian carp (*Carassius carassius*), turtles constitutively express particularly high levels of antioxidant defence systems (Bickler and Buck, 2007), although total glutathione (Willmore and Storey, 1997a) and catalase activity (Willmore and Storey, 1997b) decrease in the turtle heart during long-term anoxia. It remains unknown whether preventing ROS generation upon reoxygenation is also part of the adaptive strategy of turtles to avoid oxidative damage upon anoxia and reoxygenation.

ROS are produced by electron transfer from electron transport chain complexes (Murphy, 2009). These can be assembled in 'supercomplexes', which is claimed to affect electron transport but by unclear mechanisms (Lopez-Fabuel et al., 2016; Maranzana et al., 2013; Milenkovic et al., 2017). A major source of ROS in the mouse heart after ischemia and reperfusion is complex I of the mitochondrial electron transport chain (Chouchani et al., 2016; Galli and Richards, 2014; Murphy, 2009; Murphy and Steenbergen, 2008). During ischemia, succinate accumulates in the heart and at reperfusion it acts as a source of electrons driving reverse electron transfer (RET), where electrons are passed from succinate to the ubiquinone pool via complex II and further on to complex I

working in reverse, utilising the elevated proton motive force to generate ROS (Chouchani et al., 2016; Murphy, 2009). When complex I is inhibited by S-nitrosation, i.e. the post-translational modification of a Cys thiol by nitrosonium (NO<sup>+</sup>), ROS production is also inhibited (Chouchani et al., 2013; Lesnefsky et al., 2004; Shiva et al., 2007). In turtles acclimated to prolonged anoxia at 5°C, mimicking natural seasonal acclimation, overall levels of S-nitrosation in the heart increase dramatically, from nanomolar up to 2 μmol l<sup>-1</sup> (Jensen et al., 2014), suggesting that S-nitrosation, like other nitric oxide (NO) metabolites, could contribute to cardioprotection in turtles experiencing anoxia and reoxygenation (Fago and Jensen, 2015; Flögel et al., 2010; Jacobsen et al., 2012). Although previous studies have found a low aerobic capacity in isolated heart (Galli et al., 2013) and brain (Pamenter et al., 2016) mitochondria from anoxia-acclimated turtles, it is not known whether complex I inhibition by S-nitrosation is involved and/or if ROS generation is decreased.

Here, we test the hypothesis that the heart mitochondria of turtles exposed to prolonged anoxia reduce ROS generation compared to normoxic controls and investigate the role of complex I S-nitrosation in this response. We first investigated *in situ* perfused turtle heart performance and tissue viability following an anoxia and reoxygenation protocol. We then tested whether turtle complex I can be S-nitrosated and whether this inhibits its activity and ROS production *in vitro*. To assess the relevance *in vivo*, we then exposed cold-acclimated turtles to anoxia and normoxia and examined the effect of anoxia on ROS production and respiration rate of isolated heart mitochondria and on complex I S-nitrosation, NADH-reductase activity, level of expression and organization into mitochondrial supercomplexes.

## Materials and methods

### Chemicals

All chemicals from Sigma-Aldrich. Amplex UltraRed was from ThermoFisher Scientific and Cy3 maleimide from GE Healthcare Life Sciences.

### Animals

Red-eared sliders (*Trachemys scripta elegans*) were obtained from Lemberger Reptiles (Oshkosh, WI, USA) and allowed to recover for 4 weeks before acclimation. Turtles were kept at 25°C in large aquaria with free access to dry platforms under infrared lamps for behavioural thermoregulation. All turtles were euthanized by injection of an overdose pentobarbital (50 mg kg<sup>-1</sup>) into the supravertebral venous sinus. When the turtles were unresponsive to pinching of the legs and to the corneal reflex after 1-5 minutes, the head was cut off and the brain destroyed before the plastron was opened using a bonesaw and the ventricle removed. The whole procedure from anesthesia to heart extraction typically lasted ~5 minutes. All procedures were performed in accordance with laws of animal care and experimentation in Denmark under the permit 2015-15-0201-00544.

### *In situ* perfused heart

To assess whether the turtle heart is damaged by anoxia and reoxygenation, we kept *in situ* perfused turtle hearts (N=6, 0.549±0.036 kg) anoxic for 60 min followed by 60 min of reoxygenation at 25°C and assessed turtle heart dynamics and tissue damage, as described below. Details of this preparation are described elsewhere (Farrell et al., 1994; Joyce et al., 2016).

Briefly, turtles were anesthetized with pentobarbital (50 mg kg<sup>-1</sup>) before the plastron was removed with a bone saw. The sinus venosus and left aortic arch were cannulated with double-bore stainless steel cannulae, which permitted pressures to be measured at the tip of insertion via a PE-50 cannula. All other vessels were ligated with 4-0 surgical silk. This mimicked anoxic conditions when submerged turtles bypass the lungs by right-to-left shunting, sending the ventricular blood flow to the systemic circulation only (Hicks and Wang, 1998), which makes this setup an

appropriate model of turtle heart perfusion during anoxic breath hold. After surgery, the preparation was placed in an organ bath with saline (0.9% NaCl) kept at 25°C, and the heart was perfused with turtle Ringer solution (in mmol l<sup>-1</sup>: 80 NaCl, 40 NaHCO<sub>3</sub>, 1 NaH<sub>2</sub>PO<sub>4</sub>, 2.5 KCl, 1 MgSO<sub>4</sub>, 2 CaCl<sub>2</sub>, 5 glucose) continuously bubbled with 2% CO<sub>2</sub>, 48% N<sub>2</sub> and 52% O<sub>2</sub> (normoxia) or 2% CO<sub>2</sub>, 98% N<sub>2</sub> (anoxia). The input cannula was attached to a constant pressure filling pressure device, which could be manipulated to alter preload, and the output cannula was attached to a movable pressure head (Joyce et al., 2016). The pressure cannulae were attached to pressure transducers (PX600; Baxter Edwards, Irvine, CA, USA). Flow was measured in the output tract with an in-line Transonic flow probe (4 mm diameter; model 4NRB; Transonic System, NY, USA) and connected to a Transonic T206 flow meter. The output signals from the pressure transducers and flow meter were recorded by a Biopac MP100 data acquisition system (Biopac Systems, Goleta, CA, USA) and stored on a computer. Initial preload pressure was set to achieve a maximal flow and afterload pressure was set to ~3 kPa to mimic *in vivo* values for turtles (Joyce and Wang, 2014; Overgaard et al., 2002). After 30 min at normoxia, the gas pump settings were changed to achieve anoxia, bubbling both Ringer and the saline bath with the gas mixture to ensure anoxia in the heart. The heart was kept under anoxia for 60 min. The hearts were then reoxygenated by changing the pump settings back to the normoxic setting for 60 min.

At the end of the experiment, to visualize dead/live cardiac tissue, hearts were excised, cut into ~1 mm sections, incubated in 1% triphenyl-tetrazolium chloride (TTC) in PBS for 20 min at 25°C and fixed in 4% formalin for 24 h. Sections were placed on a black background and photographed with a Moticam 1000 1.3 megapixel microscope camera (Motic, Hong Kong) fitted on a SZ-40 Olympus microscope with 1.5x magnification. The pictures were captured with the Motic Images Plus 2.0 software, and the TIFF files were then analysed in Photoshop TM (Adobe), as described (Nadtochiy et al., 2011).

### **Thermal acclimation and exposure to normoxia and anoxia**

Turtles of similar size were fasted and gradually acclimated to 5°C over 6 weeks and then exposed to 9 days of anoxia (N=5, 0.514±0.039 kg) or normoxia (N=5, 0.526±0.031 kg), following a previously described acclimation protocol (Jensen et al., 2014). Turtles exposed to anoxia were comatose and unresponsive on the day of experimentation, but reacted to handling by withdrawing limbs.

### **Preparation of heart mitochondria from cold-acclimated turtles exposed to normoxia and anoxia**

The heart ventricle was divided in two parts, and mitochondria were isolated separately. One part was used to identify S-nitrosated (SNO) mitochondrial complexes by tagging with the fluorescent probe Cy3. In these experiments, mitochondria were isolated in STE buffer (Sigma Aldrich) (in mmol l<sup>-1</sup>: 250 sucrose, 5 Tris, 1 EGTA, 0.1 DTPA, 0.1 µmol l<sup>-1</sup> neocuproine, pH 7.4 at 4°C) with 0.5% BSA and 10 mmol l<sup>-1</sup> N-ethylmaleimide (NEM) before tagging with Cy3 as described below. NEM blocks free Cys thiols, and thereby diminishes transnitrosation and loss of endogenous S-nitrosation. The other part of ventricle was used for measuring enzymatic activity of complex I, citrate synthase activity, respiration rate and ROS (detected as H<sub>2</sub>O<sub>2</sub>) production. In these experiments, mitochondria were isolated in STE buffer with 0.5% BSA but without NEM and stored on ice in dim light (to preserve labile, light sensitive SNO) before measurements of enzyme activity, respiration rates and ROS. In order to preserve endogenous SNO, all steps were conducted as quickly as possible and in dim light.

Mitochondria were isolated from the two ventricle portions in parallel. Connective tissue was removed by dissection, the heart ventricle was cut into pieces with a razorblade and then homogenised for 5 s with an UltraTurrax homogeniser on ice. The homogenates were centrifuged at 700 g for 5 min at 4°C and the supernatants filtered through two layers of cheesecloth. The remaining pellets were then resuspended and centrifuged at 700 g for 5 min at 4°C, and the supernatants filtered again. The supernatants were then centrifuged at 10000 g for 10 min at 4°C

and the pelleted mitochondrial fractions were resuspended in a small volume of STE without BSA, with and without 10 mmol l<sup>-1</sup> NEM. Protein content of mitochondrial solutions was determined with the Pierce 660 nm Protein Assay using BSA as a standard.

### **Preparation of heart mitochondria from warm normoxic turtles and S-nitrosation by MitoSNO**

In these experiments, normoxic turtles kept at 25°C (from here on defined as warm normoxic turtles) were used to examine *in vitro* effects of S-nitrosation by MitoSNO on mitochondrial complex I activity, respiration rate and ROS production. Heart ventricle from turtles (N=5, 0.463±0.058 kg) kept at 25°C were removed and homogenised as described above in STE buffer with 0.5% BSA. The homogenate was centrifuged for 10 min at 700 g at 4°C and the supernatant was poured through two layers of cheese cloth into a new centrifuge tube and centrifuged twice at 10000 g for 10 min at 4°C. The light halo of damaged mitochondria surrounding the darker pellet of intact mitochondria was carefully removed by rinsing with buffer with a pipette before resuspension. After the final centrifugation step, the mitochondrial pellet was resuspended in a small volume of STE buffer without BSA.

Mitochondria were then incubated in KCl buffer (in mmol l<sup>-1</sup>: 120 KCl, 1 EDTA, 10 HEPES, 1% Chelex-100, pH 8.0) for 20 min before adding 50 µmol l<sup>-1</sup> of the S-nitrosating agent MitoSNO (dissolved in ethanol), the non-S-nitrosating vehicle MitoNAP (control, dissolved in ethanol) or water (control) and incubated for 1 hour at 25°C in the dark. Reversibility of S-nitrosation was tested by incubating mitochondria with 0.3 mmol l<sup>-1</sup> DTT.

### **Complex I activity**

Complex I activity was assayed as the rotenone-sensitive decrease in NADH absorbance difference at 340-380 nm at 30°C on a UV-Vis diode array spectrophotometer (Agilent 8453). Mitochondria (50 µg protein) were suspended in 1 mL complex I assay buffer (in mmol l<sup>-1</sup>: 120 KCl, 1 EDTA, 10 HEPES, pH 7.4) with 100 µmol l<sup>-1</sup> NADH, 65 µmol l<sup>-1</sup> ubiquinone Q1, 300 nmol l<sup>-1</sup> antimycin A (to inhibit complex III), 2 µmol l<sup>-1</sup> KCN (to inhibit complex IV) and 10 µg mL<sup>-1</sup> alamethicin (to permeabilise the membrane). Background rate was measured in the presence of 8 µg mL<sup>-1</sup> rotenone (to inhibit complex I).



### Citrate synthase activity

Citrate synthase activity was assayed as the formation of 2-nitro-5-thiobenzoic acid (TNB) product at 412 nm ( $\epsilon = 13600 \text{ M}^{-1} \text{ cm}^{-1}$ ) over time by UV-Vis spectroscopy as described (Srere, 1969). Mitochondria were incubated in buffer (100 mmol l<sup>-1</sup> Tris HCl, pH 8.0) with 0.1% (v/v) Triton-X-100, 370  $\mu\text{mol l}^{-1}$  acetyl CoA and 100  $\mu\text{mol l}^{-1}$  5,5'-Dithiobis(2-nitrobenzoic acid) (DTNB) substrate at 30°C. Background activity was measured before 66  $\mu\text{mol l}^{-1}$  oxaloacetate was added to initiate the reaction.

### Complex I detection by western blot

Frozen heart samples were homogenised in four-fold volume/weight ratio homogenisation buffer (100 mmol l<sup>-1</sup> Tris HCl, 1 mmol l<sup>-1</sup> EDTA, 2 mmol l<sup>-1</sup> 4-(2-aminoethyl)benzenesulfonyl fluoride, 0.3  $\mu\text{mol l}^{-1}$  aprotinin, 130  $\mu\text{mol l}^{-1}$  bestatin, 14  $\mu\text{mol l}^{-1}$  E-64, 1  $\mu\text{mol l}^{-1}$  leupeptin, 0.1% SDS, pH 7.5) and centrifuged at 16000 g for 3 min at 4°C. Supernatants were transferred and protein content was determined with a Pierce 660 nm protein assay with BSA as standard. Laemmli buffer with 50 mmol l<sup>-1</sup> reducing agent DTT was added and samples were denatured for 5 min at 95°C. Samples (50  $\mu\text{g}$  protein each lane) were loaded on an 10% Mini-PROTEAN TGX precast SDS-polyacrylamide gel (BioRad) and electrophoresed for 90 min at 100 V. Proteins were then blotted to a PVDF membrane (BioRad) on a Trans-Blot semi-dry transfer cell (BioRad) at 25V for 7 min. The membrane was blocked in Odyssey blocking buffer (LI-COR Biotechnology, Lincoln NE, USA) for 1 h and incubated overnight with 1:1000 primary mouse NDUSF3 antibody (Abcam) in Odyssey blocking buffer. The following day, the blot was rinsed in PBS + 0.02% Tween-20 and incubated with 1:10000 secondary goat anti-mouse antibody (IRDye 800CW, LI-COR Biotechnology), and developed for near-infrared fluorescence on an Odyssey Fc imaging system (LI-COR Biotechnology). The membrane was then stripped with 0.1 mol l<sup>-1</sup> NaOH and incubated with 1:5000 primary mouse GAPDH antibody (Abcam) in Odyssey blocking buffer overnight and developed with secondary antibody, as described above.

## Respiration rate and ROS production

Respiration rate and ROS production of heart mitochondria were measured in parallel in the two separate chambers of an Oroboros Oxygraph 2-k high-resolution respirometry system fitted with an O2k-fluorescence LED2-module with filters specific for detection of the Amplex UltraRed product resorufin (Oroboros Instruments, Innsbruck, Austria). The O<sub>2</sub>-electrodes were calibrated with air-saturated respiration medium (in mmol l<sup>-1</sup>: 110 sucrose, 20 taurine, 10 KH<sub>2</sub>PO<sub>4</sub>, 20 HEPES, 60 K-MES, 1.4 MgCl<sub>2</sub>, 0.5 EGTA, 0.5% BSA, pH 7.4, adjusted with 5 mol l<sup>-1</sup> KOH) and Amplex UltraRed assay reagents (10 μM Amplex UltraRed, 1 U/mL horse radish peroxidase, 20 U/mL superoxide dismutase) were added to measure H<sub>2</sub>O<sub>2</sub> generation. This method is specific for detection of H<sub>2</sub>O<sub>2</sub> in isolated mitochondria, without appreciable interference from other oxidation products (Kalyanaraman et al., 2012). Mitochondria (62 μg protein mL<sup>-1</sup>) were added to the chambers, and the O2k-fluorometer was calibrated with injections of 0.1 μmol l<sup>-1</sup> H<sub>2</sub>O<sub>2</sub> in the presence of mitochondria, to correct for ROS scavenging properties of the mitochondria. All measured respiration rates were corrected for non-mitochondrial respiration by subtracting respiration rate with 2.5 μmol l<sup>-1</sup> antimycin A, a complex III inhibitor.

Mitochondria isolated from hearts of warm normoxic turtles were used to detect whether S-nitrosation by MitoSNO affects ROS production and respiration rate. In these experiments, 5 mmol l<sup>-1</sup> succinate was added to the Oxygraph chambers at 25°C to initiate state II respiration (i.e. respiration in the absence of added ADP) and ROS production via RET and the mitochondria were allowed to respire to anoxia. The mitochondria were then left under anoxia for 30 min, and 50 μmol l<sup>-1</sup> MitoSNO, MitoNAP (vehicle, control) or 10 μL H<sub>2</sub>O (control) was added 5 min before reoxygenation. The chambers were reoxygenated for 2 min by lifting the stoppers of the chambers and ROS production and respiration rates were again measured. The complex I inhibitor rotenone (8 μg mL<sup>-1</sup>) was added to measure non-complex I ROS production and respiration rate.

Mitochondria isolated from hearts from cold-acclimated normoxic and anoxic turtles were exposed to two different protocols run in parallel in the two chambers. In one chamber, ROS production from RET was induced by adding 5 mmol l<sup>-1</sup> succinate. This reflects the maximal

capacity for ROS production and respiration with succinate. Rotenone ( $8 \mu\text{mol l}^{-1}$ ), an inhibitor of complex I, was then added to measure non-complex I ROS production and respiration rate. Afterwards,  $1 \text{ mmol l}^{-1}$  ADP was added to induce maximal (complex II-dependent) respiration rate (i.e. state III respiration, under phosphorylating conditions). In the other chamber, malate ( $2.5 \text{ mmol l}^{-1}$ ) and pyruvate ( $5 \text{ mmol l}^{-1}$ ) were added and complex I-dependent state II respiration rate was recorded. ADP ( $1 \text{ mmol l}^{-1}$ ) was then added to initiate complex I-dependent state III respiration rate, and succinate ( $5 \text{ mmol l}^{-1}$ ) was added to measure state III respiration rate dependent on both complex I and II. An increase of less than 10% in respiration rate after addition of cytochrome c ( $10 \mu\text{mol l}^{-1}$ ) was taken as a proof that the mitochondria were intact (Galli et al., 2013). The mitochondria were finally uncoupled with titrations of carbonyl cyanide-*p*-tri-fluoromethoxyphenylhydrazone (FCCP, dissolved in ethanol) to assess maximal respiration rate. Assuming identical temperature effects on mitochondrial function of normoxic and anoxic turtles, as determined in previous studies (Galli and Richards, 2012), respiration rate and ROS production were measured at  $20^\circ\text{C}$  instead of the acclimation temperature at  $5^\circ\text{C}$ , as the lower respiration rate would prolong the protocol duration.

### **Detection of S-nitrosothiols by Cy3 fluorescent labelling in BN-PAGE and complex I identification**

S-nitrosated mitochondrial complexes (from cold-acclimated turtles exposed to anoxia and normoxia and from warm normoxic turtles) were selectively labelled with fluorescent Cy3-maleimide and detected by Blue Native-PAGE (BN-PAGE) as described (Chouchani et al., 2013). Briefly, mitochondria were isolated in STE buffer with  $10 \text{ mmol l}^{-1}$  NEM as described above and lysed before free thiols were blocked with  $10 \text{ mmol l}^{-1}$  NEM for 10 min at  $25^\circ\text{C}$ . Excess NEM was then removed by washing with NEM-free PBS buffer with 1% chelex-100, followed by centrifugation. Upon the final resuspension, S-nitrosothiols were selectively reduced with  $1 \text{ mmol l}^{-1}$  ascorbate and  $10 \mu\text{mol l}^{-1}$   $\text{CuSO}_4$  and then tagged with  $40 \mu\text{M}$  Cy3-maleimide for 30 min at  $25^\circ\text{C}$ , in the dark. Mitochondrial membrane proteins were extracted with dodecyl maltoside (DDM) and separated by BN-PAGE and scanned for Cy3 fluorescence using a 532 nm laser and a 580 nm emission filter (band pass of 30 nm) on a Typhoon 9410 molecular imager (GE Healthcare). Mouse heart mitochondria were isolated as described for warm normoxic turtles and loaded onto BN-PAGE as a marker to identify bands. Intensity of bands were quantified relative to the protein stain

of the complex V band with the ImageJ (version 1.51m9, NIH, Bethesda, MD, USA) Gel Analysis method. Because the protein stain of some of the bands with complex I activity was too weak to quantify (in particular the LW-CI band), the complex V band was used as a reference as the complex V protein level does not change with exposure to anoxia in turtles (Galli et al., 2013; Pamerter et al., 2016) and thus can serve as a relative loading control.

Bands with complex I activity were identified in BN-PAGE by incubation of the gels with  $150 \mu\text{mol l}^{-1}$  NADH and  $1 \text{ mg mL}^{-1}$  nitroblue tetrazolium. Presence of NADH-reductase activity of bands was detected as a purple staining (Van Coster et al., 2001).

### Statistics

Significant differences between treatments were assessed with two-way repeated measures ANOVA with Sidak's correction for multiple testing. Statistical significance was set to  $P < 0.05$ . Statistical analysis was performed in Prism (version 7.0c, Graphpad Software Inc., La Jolla, CA, USA). All data are reported as means  $\pm$  SEM.

### Results

Turtle heart function, assessed by flow, power and stroke volume in an *in situ* perfused heart, decreased during 60 min anoxia but fully recovered at reoxygenation (Fig. 1A). Accordingly, dead ventricular tissue assessed by TTC staining after anoxia and reoxygenation (Fig. 1B,C) was very low ( $2.41 \pm 0.34\%$ ,  $N=6$ ), showing the extraordinary tolerance to prolonged anoxia followed by reoxygenation of the turtle heart. To understand if this tolerance was due to a low mitochondrial ROS production, we isolated heart mitochondria from cold-acclimated turtles exposed to anoxia or normoxia and measured respiration rate and ROS production in the presence of succinate and low ADP, conditions favouring RET and ROS generation (Chouchani et al., 2016; Murphy, 2009). We found that heart mitochondria from anoxic turtles produced significantly less ROS and have lower aerobic capacity than those from normoxic ones (Fig. 2A-D). In addition, ROS production was almost completely abolished by rotenone, an inhibitor of complex I, indicating that complex I is the main source of mitochondrial ROS with succinate as the substrate (Fig. 2A-C). Addition of ADP

– leading to dissipation of the H<sup>+</sup> electrochemical potential gradient through complex V and favouring forward electron transfer – initiated state III respiration and almost completely reduced all remaining ROS production (Fig. 2A-C). Interestingly, heart mitochondria state III respiration rate induced by ADP was significantly lower in mitochondria from anoxic than in normoxic turtles (Fig. 2D). Parallel experiments confirmed significantly lower respiration rates of heart mitochondria from anoxic turtles also with pyruvate and malate as substrates (i.e. under complex I-dependent conditions), in the absence (state II) and presence (state III) of added ADP, and when the mitochondria were fully uncoupled with FCCP to yield maximal respiration rate (Fig. 2E). Citrate synthase activity of heart mitochondria was significantly lower in anoxic than in normoxic turtles (Fig. 2F). Taken together, these data show consistently lower respiration rates and aerobic capacity of heart mitochondria from anoxic turtles compared to normoxic ones.

We then investigated if the decrease in ROS production in anoxic turtle mitochondria (Fig. 2C) was due to S-nitrosation of complex I (Fig. 3A), which is the main ROS producing site (Fig. 2C). To verify that complex I is a potential target of S-nitrosation in the turtle heart, we first used isolated heart mitochondria from warm normoxic turtle to measure complex I NADH-reductase activity and ROS production after treatment with a mitochondria-targeted S-nitrosating agent, MitoSNO.

Incubation with MitoSNO almost abolished complex I activity (Fig. 3B), an effect that was partially reversed by addition of the thiol reducing agent DTT (Fig. 3B), which cleaves the S-NO bond. MitoSNO also significantly lowered succinate-dependent ROS production after exposing mitochondria to anoxia and reoxygenation (Fig. 3C,E), while leaving respiration rate unaffected (Fig. 3F). The control compound, MitoNAP or vehicle, had no effects (Fig. 3D,E). Addition of the complex I inhibitor rotenone significantly decreased ROS production in all groups (Fig. 3E) without large changes in respiration rate (Fig. 3F), confirming RET through complex I as a major potential source of ROS in turtle heart mitochondria after anoxia and reoxygenation *in vitro* (Fig. 3A,C).

Having established that turtle complex I can be S-nitrosated and that this S-nitrosation inhibits activity and ROS production *in vitro*, we then investigated whether the depression of respiration rate and ROS generation observed in heart mitochondria from turtles exposed to anoxia (Fig. 2) could be ascribed to complex I S-nitrosation. To do this, complex I in heart mitochondria from cold-acclimated (anoxic and normoxic) and warm normoxic turtles was identified by an in-gel activity stain on BN-PAGE (Fig. 4). Visualization of mitochondrial S-nitrosation by Cy3-tagging

revealed a highly similar pattern of S-nitrosation of mitochondrial complexes in anoxic and normoxic turtles, with three major S-nitrosated bands corresponding to two bands with complex I activity (of higher and lower molecular mass than predicted) and a band corresponding to complex V (ATP synthase). There was no difference in the extent of S-nitrosation of mitochondrial complexes, as estimated from the intensity of these bands, between anoxic and normoxic turtles (Fig. 4B).

Complex I activity in anoxic turtles was similar to that in normoxic ones and, in contrast to treatment with MitoSNO, the activity could not be increased by DTT (Fig. 5A). Complex I protein expression examined by western blot was also not different in anoxic turtles (Fig. 5C,D), consistent with activity data (Fig. 5A).

Interestingly, most of complex I in turtle heart mitochondria appears consistently arranged in high molecular weight supercomplexes. This is shown by several high molecular mass bands with NADH reductase activity on BN-PAGE gels (Fig. 4) that are present even when mitochondria are treated with the detergent dodecyl maltoside (DDM), which dissolves mitochondrial supercomplexes in mammals (Milenkovic et al., 2017). In contrast to turtle, mouse heart mitochondria show a single, well-defined band with complex I activity (Fig. 4A). Turtle supercomplexes do not seem to be stabilised by disulphide bonds as they were still present after treatment with DTT (data not shown). However, incubation of turtle mitochondria with NEM to alkylate free Cys partly breaks up supercomplexes and creates a low molecular weight band with NADH-reductase activity (indicated by LW-CI in Fig. 4A), suggesting that this band likely represents the flavin-containing matrix-arm of complex I. This band was the most intensively Cy3-labelled in heart mitochondria from cold-acclimated turtles, indicating that this part of complex I is a major S-nitrosation site in turtles (Fig. 4B). Several S-nitrosated Cys residues have previously been detected in this part of complex I in mouse but without apparent effects on activity (Chouchani et al., 2013; Chouchani et al., 2017). In addition, we observed strong labelling of complex V even in the absence of MitoSNO and a slight S-nitrosation of complex I in the supercomplex high-molecular weight form (Fig. 4). S-nitrosation does not affect complex V activity in mammals (Chouchani et al., 2013; Prime et al., 2009).

## Discussion

Freshwater turtles are remarkable among vertebrates in their ability to survive prolonged anoxia and to avoid oxidative damage by a range of physiological adaptations. The turtle heart is particularly noteworthy in that it keeps pumping blood – albeit at a very low rate – in the complete absence of oxygen and fully recovers at reoxygenation (Overgaard et al., 2007; Stecyk et al., 2009; Wasser, 1996). Even after prolonged oxygen deprivation, turtles almost immediately recover arterial oxygenation when they regain access to air (Jacobsen et al., 2012; Ultsch and Jackson, 1982), exposing themselves to the risk of oxidative stress. However, as shown here (Fig. 1) and elsewhere (Wasser et al., 1992; Wasser et al., 1997), even rapid reoxygenation causes no damage to the turtle heart, although the underlying mechanisms for such extraordinary performance are still poorly understood. Here, we find that when turtles are exposed to prolonged anoxia, heart mitochondria not only decrease the aerobic capacity, confirming earlier results (Galli et al., 2013), but also ROS production (Fig. 2). We observed these effects in the presence of succinate, a key metabolite that accumulates in the heart during hypoxia in mammals (Chouchani et al., 2014) and during anoxia in turtles (A. Bundgaard and A. M. James, unpublished data; Buck, 2000). Suppression of mitochondrial ROS generation after a period of prolonged anoxia could limit oxidative stress at reoxygenation and explain the full *in situ* recovery of perfused turtle heart after 60 min of anoxia and negligible tissue damage (Fig. 1). Interestingly, the brain of anoxic turtles also shows ROS suppression (Milton et al., 2007), suggesting that this may be a common strategy of anoxia tolerance of turtle tissues.

Our results provide clues on the origin of ROS production in turtle heart mitochondria. Addition of the complex I inhibitor rotenone almost completely blocks succinate-dependent ROS generation, implicating RET from complex I as a potential major pathway of ROS production in the turtle heart (Fig. 2C). S-nitrosation of a specific Cys residue on the ND3 subunit of complex I can inhibit ROS generation during RET in mouse heart mitochondria (Chouchani et al., 2013) and protect the heart at reoxygenation (Lesnefsky et al., 2004; Shiva et al., 2007). As overall S-nitrosation is elevated in anoxic turtles (Jensen et al., 2014), we investigated whether this modification could contribute to the high tolerance of the turtle heart to anoxia and reoxygenation. We found that turtle complex I can be S-nitrosated *in vitro* by MitoSNO with potent reduction of complex I enzymatic activity (Fig. 3A) and ROS generation (Fig. 3C). However, while S-nitrosation of complex I could be detected in

mitochondria isolated from normoxic and anoxic turtles (Fig. 4,5), indicating that S-nitrosation occurs *in vivo* and at specific mitochondrial targets (Foster et al., 2009). However, the decrease in ROS observed in heart mitochondria from anoxic turtles compared to normoxic ones (Fig. 2C) cannot be ascribed to this protein modification, as complex I shows similar SNO levels (Fig. 4B), enzymatic activity that was unaffected by thiol reduction with DTT (Fig. 5A) and levels of expression (Fig. 5B,C). In conclusion, S-nitrosation of complex I does not appear to be involved in how the turtle heart is protected from oxidative damage after anoxia and reoxygenation. Instead, our results indicate that mitochondria produce less ROS when isolated from anoxic turtles and that this effect is associated with a generalized decrease in mitochondrial aerobic capacity (Fig. 2). Inhibition of complex V during anoxia would contribute to reduce aerobic capacity by maintaining a high proton electrochemical potential gradient across the inner mitochondrial membrane and consequently by decreasing electron flow in the respiratory chain (Galli et al., 2013). However, these effects would also favour reverse electron and proton transfer through complex I and increase ROS, which is not supported by our data (Fig. 2A-C). Instead, the decrease in citrate synthase activity in anoxic turtle mitochondria (Fig. 2F) suggests a general reduction in the expression of mitochondrial proteins, reflecting protein synthesis arrest (Boutilier and St-Pierre, 2000), or increased enzyme inhibition. However, a previous study (Galli et al., 2013) has reported similar citrate synthase activities in normoxic and anoxic turtle heart mitochondria, but much lower than those measured here, perhaps due to the use of a different protocol (Galli et al., 2016). Low ROS production seems to be a general adaptation upon acclimation to low oxygen in ectotherms such as killifish (Du et al., 2016; Duerr and Podrabsky, 2010), shovelnose rays (Hickey et al., 2012) and epaulette sharks (Hickey et al., 2012), but the mechanisms remain elusive. In the turtle, the *in vivo* mitochondrial ROS production at reoxygenation in the spring after winter anoxia will depend on numerous factors, including levels of ADP (Fig. 2C), rate of tissue reoxygenation (that can be modulated by cardiac shunting (Williams and Hicks, 2016)) and temperature. In contrast, mitochondrial ROS scavenging capacity is independent on anoxia acclimation in turtles, having constitutively high activities of the ROS scavenging enzymes catalase, superoxide dismutase, glutathione peroxidase and alkyl hydroperoxide reductase (Willmore and Storey, 1997b) and glutathione levels (Willmore and Storey, 1997a). Experiments are underway in our



group to determine endogenous levels of ROS following anoxia and reoxygenation in turtles *in vivo*, as done with other species (Cochemé et al., 2012; Salin et al., 2017).

A surprising finding of this study is that turtle complex I appears to be arranged in supercomplexes with other respiratory complexes (Fig. 4). Turtle supercomplexes appear more stable to detergents than those in mammalian mitochondria, as found in the mouse (Lapiente-Brun et al., 2013), pig (Wu et al., 2016), sheep (Letts et al., 2016) and cow (Althoff et al., 2011; Shinzawa-Itoh et al., 2016), possibly due to different fatty acid compositions of the inner mitochondrial membrane in ectotherms compared to endotherms (Brand et al., 1991; Brookes et al., 1998). Although the role of supercomplexes is unclear and disputed, it has been proposed that they may limit ROS production (Lopez-Fabuel et al., 2016; Maranzana et al., 2013). Whether this may be another factor contributing to the extraordinary tolerance to anoxia and reoxygenation of turtles is an intriguing possibility.

In conclusion, while anoxia both decreases mitochondrial ROS production and respiration rate, and elevates general S-nitrosation, the reversible S-nitrosation of complex I does not contribute to the protection of the turtle heart against reoxygenation injury. The mechanisms of this protection will need to be clarified in future studies.

## References

- Althoff, T., Mills, D. J., Popot, J.-L. and Kühlbrandt, W.** (2011). Arrangement of electron transport chain components in bovine mitochondrial supercomplex I<sub>1</sub>III<sub>2</sub>IV<sub>1</sub>. *EMBO J.* **30**, 4652–4664.
- Bickler, P. E. and Buck, L. T.** (2007). Hypoxia tolerance in reptiles, amphibians, and fishes: Life with variable oxygen availability. *Annu. Rev. Physiol.* **69**, 145–170.
- Boutilier, R. G. and St-Pierre, J.** (2000). Surviving hypoxia without really dying. *Comp. Biochem. Physiol. - A Mol. Integr. Physiol.* **126**, 481–490.
- Brand, M. D., Couture, P., Else, P. L., Withers, K. W. and Hulbert, A. J.** (1991). Evolution of energy-metabolism - Proton permeability of the inner membrane of liver-mitochondria is greater in a mammal than in a reptile. *Biochem. J.* **275**, 81–86.
- Brookes, P. S., Buckingham, J. A., Tenreiro, A. M., Hulbert, A. and Brand, M. D.** (1998). The proton permeability of the inner membrane of liver mitochondria from ectothermic and endothermic vertebrates and from obese rats: Correlations with standard metabolic rate and phospholipid fatty acid composition. *Comp. Biochem. Physiol. Part B Biochem. Mol. Biol.* **119**, 325–334.
- Buck, L. T.** (2000). Succinate and alanine as anaerobic end-products in the diving turtle (*Chrysemys picta bellii*). *Comp. Biochem. Physiol. - B Biochem. Mol. Biol.* **126**, 409–413.
- Chouchani, E. T., Methner, C., Nadtochiy, S. M., Logan, A., Pell, V. R., Ding, S., James, A. M., Cochemé, H. M., Reinhold, J., Lilley, K. S., et al.** (2013). Cardioprotection by S-nitrosation of a cysteine switch on mitochondrial complex I. *Nat. Med.* **19**, 753–9.
- Chouchani, E. T., Pell, V. R., Gaude, E., Akseptijević, D., Sundier, S. Y., Robb, E. L., Logan, A., Nadtochiy, S. M., Ord, E. N. J., Smith, A. C., et al.** (2014). Ischaemic accumulation of succinate controls reperfusion injury through mitochondrial ROS. *Nature* **515**, 431–435.
- Chouchani, E. T., Pell, V. R., James, A. M., Work, L. M., Saeb-Parsy, K., Frezza, C., Krieg, T. and Murphy, M. P.** (2016). A unifying mechanism for mitochondrial superoxide production during ischemia-reperfusion injury. *Cell Metab.* **23**, 254–263.
- Chouchani, E. T., James, A. M., Methner, C., Pell, V. R., Prime, T. A., Erikson, B. K., Forkink, M., Lau, G. Y., Bright, T. P., Menger, K. E., et al.** (2017). Identification and quantification of protein S-nitrosation by nitrite in the mouse heart during ischemia. *J. Biol. Chem.* jbc.M117.798744.
- Cochemé, H. M., Logan, A., Prime, T. A., Abakumova, I., Quin, C., McQuaker, S. J., Patel, J. V., Fearnley, I. M., James, A. M., Porteous, C. M., et al.** (2012). Using the mitochondria-targeted ratiometric mass spectrometry probe MitoB to measure H<sub>2</sub>O<sub>2</sub> in living *Drosophila*. *Nat. Protoc.* **7**, 946–958.
- Du, S. N. N., Mahalingam, S., Borowiec, B. G. and Scott, G. R.** (2016). Mitochondrial physiology and reactive oxygen species production are altered by hypoxia acclimation in killifish (*Fundulus heteroclitus*). *J. Exp. Biol.* **219**, 1130–1138.
- Duerr, J. M. and Podrabsky, J. E.** (2010). Mitochondrial physiology of diapausing and developing embryos of the annual killifish *Austrofundulus limnaeus*: Implications for extreme anoxia tolerance. *J. Comp. Physiol. B Biochem. Syst. Environ. Physiol.* **180**, 991–1003.
- Fago, A. and Jensen, F. B.** (2015). Hypoxia tolerance, nitric oxide, and nitrite: Lessons from extreme animals. *Physiology (Bethesda)*. **30**, 116–126.
- Farrell, A., Franklin, C., Arthur, P., Thorarensen, H. and Cousins, K.** (1994). Mechanical performance of an *in situ* perfused heart from the turtle *Chrysemys scripta* during normoxia and anoxia at 5 C and 15 C. *J. Exp. Biol.* **191**, 207–229.

- Flögel, U., Fago, A., Rassaf, T., Amelio, D., Garofalo, F., Brunelli, E., Loong, A. M., Wong, W. P., Ip, Y. K., Tota, B., et al. (2010). Keeping the heart in balance: the functional interactions of myoglobin with nitrogen oxides. *J. Exp. Biol.* **213**, 2726–33.
- Foster, M. W., Hess, D. T. and Stamler, J. S. (2009). Protein S-nitrosylation in health and disease: a current perspective. *Trends Mol. Med.* **15**, 391–404.
- Galli, G. L. J. and Richards, J. G. (2012). The effect of temperature on mitochondrial respiration in permeabilized cardiac fibres from the freshwater turtle, *Trachemys scripta*. *J. Therm. Biol.* **37**, 195–200.
- Galli, G. L. J. and Richards, J. G. (2014). Mitochondria from anoxia-tolerant animals reveal common strategies to survive without oxygen. *J. Comp. Physiol. B Biochem. Syst. Environ. Physiol.* **184**, 285–302.
- Galli, G. L. J., Lau, G. Y. and Richards, J. G. (2013). Beating oxygen: chronic anoxia exposure reduces mitochondrial F<sub>1</sub>F<sub>0</sub>-ATPase activity in turtle (*Trachemys scripta*) heart. *J. Exp. Biol.* **216**, 3283–93.
- Galli, G. L. J., Crossley, J., Elsey, R. M., Dzialowski, E. M., Shiels, H. A. and Crossley, D. A. (2016). Developmental plasticity of mitochondrial function in American alligators, *Alligator mississippiensis*. *Am. J. Physiol. - Regul. Integr. Comp. Physiol.* ajpgu.00107.2016.
- Hickey, A. J. R., Renshaw, G. M. C., Speers-Roesch, B., Richards, J. G., Wang, Y., Farrell, A. P. and Brauner, C. J. (2012). A radical approach to beating hypoxia: Depressed free radical release from heart fibres of the hypoxia-tolerant epaulette shark (*Hemiscyllium ocellatum*). *J. Comp. Physiol. B Biochem. Syst. Environ. Physiol.* **182**, 91–100.
- Hicks, J. W. and Wang, T. (1998). Cardiovascular regulation during anoxia in the turtle: An *in vivo* study. *Physiol. Zool.* **71**, 1–14.
- Hochachka, P. W., Buck, L. T., Doll, C. J. and Land, S. C. (1996). Unifying theory of hypoxia tolerance: Molecular/metabolic defense and rescue mechanisms for surviving oxygen lack. *Proc. Natl. Acad. Sci. U. S. A.* **93**, 9493–9498.
- Jackson, D. C. (2000). Living without oxygen: Lessons from the freshwater turtle. *Comp. Biochem. Physiol. Part A* **125**, 299–315.
- Jacobsen, S. B., Hansen, M. N., Jensen, F. B., Skovgaard, N., Wang, T. and Fago, A. (2012). Circulating nitric oxide metabolites and cardiovascular changes in the turtle *Trachemys scripta* during normoxia, anoxia and reoxygenation. *J. Exp. Biol.* **215**, 2560–2566.
- Jensen, F. B., Hansen, M. N., Montesanti, G. and Wang, T. (2014). Nitric oxide metabolites during anoxia and reoxygenation in the anoxia-tolerant vertebrate *Trachemys scripta*. *J. Exp. Biol.* **217**, 423–431.
- Joyce, W. and Wang, T. (2014). Adenosinergic regulation of the cardiovascular system in the red-eared slider *Trachemys scripta*. *Comp. Biochem. Physiol. -Part A Mol. Integr. Physiol.* **174**, 18–22.
- Joyce, W., Axelsson, M., Altimiras, J. and Wang, T. (2016). *In situ* cardiac perfusion reveals interspecific variation of intraventricular flow separation in reptiles. *J. Exp. Biol.* **219**,.
- Kalyanaraman, B., Darley-Usmar, V., Davies, K. J. A., Dennery, P. A., Forman, H. J., Grisham, M. B., Mann, G. E., Moore, K., Roberts, L. J., Ischiropoulos, H., et al. (2012). Measuring reactive oxygen and nitrogen species with fluorescent probes: challenges and limitations. *Free Radic. Biol. Med.* **52**, 1–6.
- Kowaltowski, A. J., de Souza-Pinto, N. C., Castilho, R. F. and Vercesi, A. E. (2009). Mitochondria and reactive oxygen species. *Free Radic. Biol. Med.* **47**, 333–343.

- Lapuente-Brun, E., Moreno-Loshuertos, R., Acín-Pérez, R., Latorre-Pellicer, A., Colás, C., Balsa, E., Perales-Clemente, E., Quirós, P. M., Calvo, E., Rodríguez-Hernández, M. a, et al. (2013). Supercomplex assembly determines electron flux in the mitochondrial electron transport chain. *Science* **340**, 1567–70.
- Lesnefsky, E. J., Chen, Q., Moghaddas, S., Hassan, M. O., Tandler, B. and Hoppel, C. L. (2004). Blockade of electron transport during ischemia protects cardiac mitochondria. *J. Biol. Chem.* **279**, 47961–47967.
- Letts, J. A., Degliesposti, G., Fiedorczuk, K., Skehel, M. and Sazanov, L. A. (2016). Purification of ovine respiratory complex I results in a highly active and stable preparation. *J. Biol. Chem.* **291**, jbc.M116.735142.
- Lopez-Fabuel, I., Le Douce, J., Logan, A., James, A. M., Bonvento, G., Murphy, M. P., Almeida, A. and Bolaños, J. P. (2016). Complex I assembly into supercomplexes determines differential mitochondrial ROS production in neurons and astrocytes. *Proc. Natl. Acad. Sci.* 201613701.
- Maranzana, E., Barbero, G., Falasca, A. I., Lenaz, G. and Genova, M. L. (2013). Mitochondrial respiratory supercomplex association limits production of reactive oxygen species from complex I. *Antioxid. Redox Signal.* **19**, 1469–80.
- Milenkovic, D., Blaza, J. N., Larsson, N.-G. and Hirst, J. (2017). The enigma of the respiratory chain supercomplex. *Cell Metab.* **25**, 765–776.
- Milton, S. L., Nayak, G., Kesaraju, S., Kara, L. and Prentice, H. M. (2007). Suppression of reactive oxygen species production enhances neuronal survival *in vitro* and *in vivo* in the anoxia-tolerant turtle *Trachemys scripta*. *J. Neurochem.* **101**, 993–1001.
- Murphy, M. P. (2009). How mitochondria produce reactive oxygen species. *Biochem. J.* **417**, 1–13.
- Murphy, E. and Steenbergen, C. (2008). Mechanisms underlying acute protection from cardiac ischemia-reperfusion injury. *Physiol. Rev.* **88**, 581–609.
- Nadtochiy, S. M., Redman, E., Rahman, I. and Brookes, P. S. (2011). Lysine deacetylation in ischaemic preconditioning: The role of SIRT1. *Cardiovasc. Res.* **89**, 643–649.
- Overgaard, J., Stecyk, J. A. W., Farrell, A. P. and Wang, T. (2002). Adrenergic control of the cardiovascular system in the turtle *Trachemys scripta*. *J. Exp. Biol.* **205**, 3335–3345.
- Overgaard, J., Gesser, H. and Wang, T. (2007). Tribute to P. L. Lutz: cardiac performance and cardiovascular regulation during anoxia/hypoxia in freshwater turtles. *J. Exp. Biol.* **210**, 1687–99.
- Pamenter, M. E., Gomez, C. R., Richards, J. G. and Milsom, W. K. (2016). Mitochondrial responses to prolonged anoxia in brain of red-eared slider turtles. *Biol. Lett.* **12**, 20150797.
- Prime, T. A., Blaikie, F. H., Evans, C., Nadtochiy, S. M., James, A. M., Dahm, C. C., Vitturi, D. A., Patel, R. P., Hiley, C. R., Abakumova, I., et al. (2009). A mitochondria-targeted S-nitrosothiol modulates respiration, nitrosates thiols, and protects against ischemia-reperfusion injury. *Proc. Natl. Acad. Sci. U. S. A.* **106**, 10764–9.
- Salin, K., Auer, S. K., Villasevil, E. M., Anderson, G. J., Cairns, A. G., Mullen, W., Hartley, R. C. and Metcalfe, N. B. (2017). Using the MitoB method to assess levels of reactive oxygen species in ecological studies of oxidative stress. *Sci. Rep.* **7**, 41228.
- Shinzawa-Ittoh, K., Shimomura, H., Yanagisawa, S., Shimada, S., Takahashi, R., Oosaki, M., Ogura, T. and Tsukihara, T. (2016). Purification of active respiratory supercomplex from bovine heart mitochondria enables functional studies. *J. Biol. Chem.* **291**, 4178–4184.
- Shiva, S., Sack, M. N., Greer, J. J., Duranski, M., Ringwood, L. a, Burwell, L., Wang, X., MacArthur, P. H., Shoja, A., Raghavachari, N., et al. (2007). Nitrite augments tolerance to

ischemia/reperfusion injury via the modulation of mitochondrial electron transfer. *J. Exp. Med.* **204**, 2089–2102.

- Stecyk, J. a W., Bock, C., Overgaard, J., Wang, T., Farrell, A. P. and Pörtner, H.-O.** (2009). Correlation of cardiac performance with cellular energetic components in the oxygen-deprived turtle heart. *Am. J. Physiol. Regul. Integr. Comp. Physiol.* **297**, R756-68.
- Ultsch, G. R.** (1989). Ecology and physiology of hibernation and overwintering among freshwater fishes, turtles, and snakes. *Biol. Rev.* **64**, 435–516.
- Ultsch, G. R. and Jackson, D. C.** (1982). Long-term submergence at 3 °C of the turtle, *Chrysemys picta bellii*, in normoxic and severely hypoxic water. *J. Exp. Biol.* **96**, 11–28.
- Van Coster, R., Smet, J., George, E., De Meirleir, L., Seneca, S., Van Hove, J., Sebire, G., Verhelst, H., De Bleecker, J., Van Vlem, B., et al.** (2001). Blue native polyacrylamide gel electrophoresis: A powerful tool in diagnosis of oxidative phosphorylation defects. *Pediatr. Res.* **50**, 658–665.
- Wasser, J. S.** (1996). Maintenance of cardiac function during anoxia in turtles: From cell to organism. *Comp. Biochem. Physiol. Part B Biochem. Mol. Biol.* **113**, 15–22.
- Wasser, J. S., Meinertz, E. a, Chang, S. Y., Lawler, R. G. and Jackson, D. C.** (1992). Metabolic and cardiodynamic responses of isolated turtle hearts to ischemia and reperfusion. *Am. J. Physiol.* **262**, 437–443.
- Wasser, J. S., Guthrie, S. S. and Chari, M.** (1997). *In vitro* tolerance to anoxia and ischemia in isolated hearts from hypoxia sensitive and hypoxia tolerant turtles. *Comp. Biochem. Physiol. Part A Physiol.* **118**, 1359–1370.
- Williams, C. L. and Hicks, J. W.** (2016). Continuous arterial PO<sub>2</sub> profiles in unrestrained, undisturbed aquatic turtles during routine behaviors. *J. Exp. Biol.* 3616–3625.
- Willmore, W. G. and Storey, K. B.** (1997a). Glutathione systems and anoxia tolerance in turtles. *Am. J. Physiol.* **273**, 219–225.
- Willmore, W. G. and Storey, K. B.** (1997b). Antioxidant systems and anoxia tolerance in a freshwater turtle *Trachemys scripta elegans*. *Mol. Cell. Biochem.* **170**, 177–185.
- Wu, M., Gu, J., Guo, R., Huang, Y., Yang, M., Acín-Pérez, R., Bayona-Bafaluy, M. P., Fernández-Silva, P., Moreno-Loshuertos, R., Pérez-Martos, A., et al.** (2016). Structure of mammalian respiratory supercomplex I<sub>1</sub>III<sub>2</sub>IV<sub>1</sub>. *Cell* **167**, 1598–1609.
- Yellon, D. M. and Hausenloy, D. J.** (2007). Myocardial reperfusion injury. *New Engl. J. Med. Rev.* **357**, 1121–1135.

## Figures

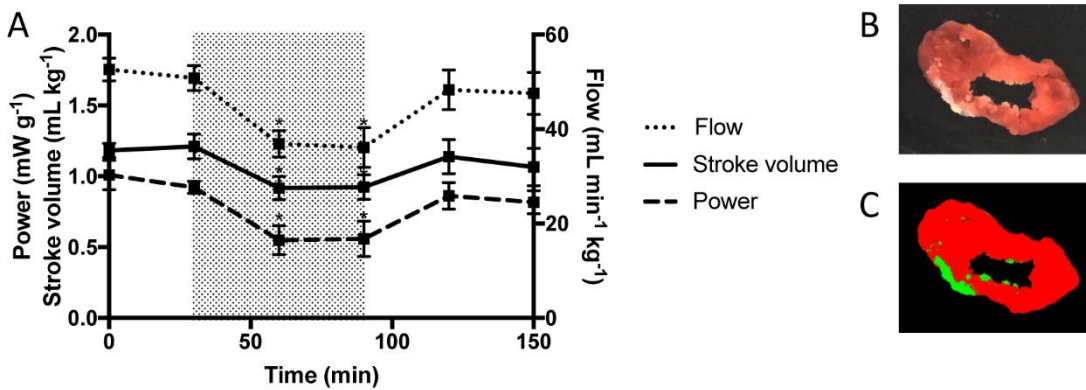


**Figure 1.** Effects of anoxia and reoxygenation on cardiac function and tissue viability of turtle heart. **A)** Flow, power output and stroke volume measured on *in situ* perfused turtle hearts exposed to 60 min anoxia (shaded area) and 60 min reoxygenation at 25°C (N=6). All cardiac function parameters were significantly decreased during anoxia (\*P<0.05). Data are shown as means  $\pm$  SEM. **B)** Representative TTC-stained ventricular section after exposure to 60 min anoxia and 60 min reoxygenation to evidence dead (white) and live (red) tissue. **C)** Representative masking of dead (green) and live (red) tissue by Photoshop™ analysis (Adobe), as described in Materials and Methods.



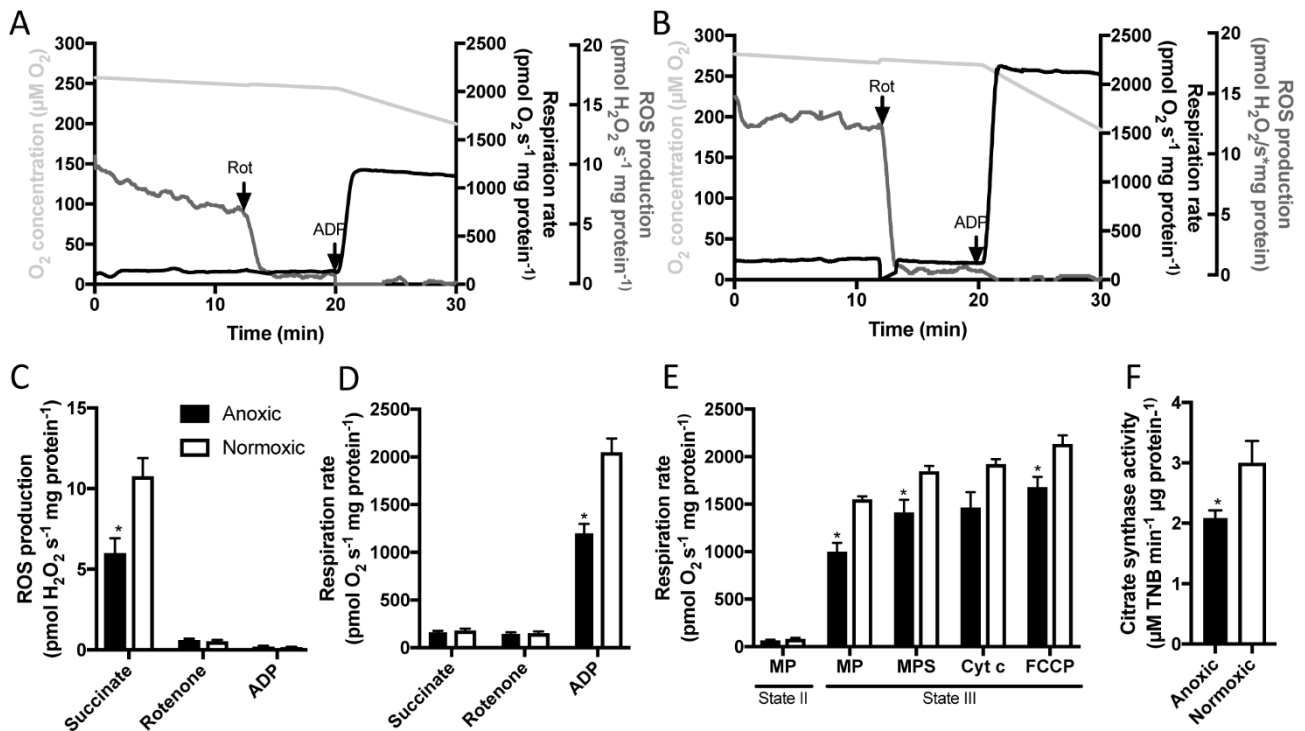


**Figure 2.** ROS production, oxygen concentration and respiration rate over time in heart mitochondria from turtles acclimated to 5°C and exposed to anoxia or normoxia. Representative traces of heart mitochondria from **A)** anoxic and **B)** normoxic turtles respiring on succinate. Addition of rotenone (Rot) and ADP is indicated. Quantification of **C)** ROS production and **D)** respiration rate of experiments performed as in A) and B) in heart mitochondria from anoxic (black bars) and normoxic (white bars) turtles (N=5 in each group). **E)** Respiration rate of anoxic and normoxic heart mitochondria run in parallel with the protocol shown in A) and B) measured in absence (state II) and presence of ADP (state III) after addition of malate (M), pyruvate (P), succinate (S), cytochrome c (cyt c) and uncoupling with FCCP (N=5 in each group). **F)** Citrate synthase activity of turtle heart mitochondria (N=5 in each group). Data are shown as means  $\pm$  SEM. Asterisks denote a significant difference between anoxic and normoxic values ( $P < 0.05$ ).

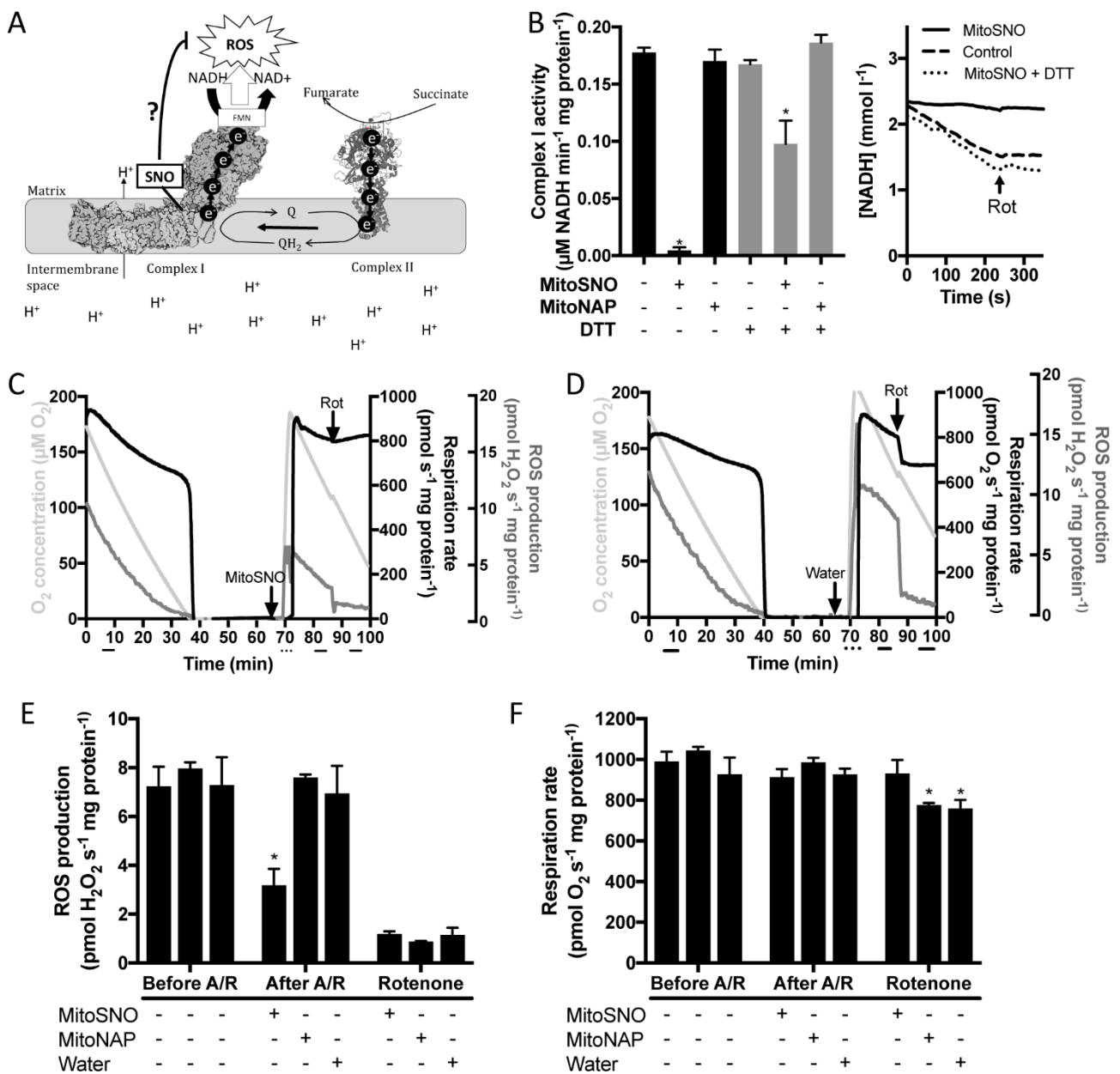


**Figure 3.** MitoSNO reversibly inhibits complex I activity and mitochondrial ROS production and respiration rate after anoxia and reoxygenation of heart mitochondria from warm normoxic turtles. **A)** Model of inhibition of complex I by S-nitrosation, preventing ROS production upon



reoxygenation by reverse electron transfer (RET) from accumulated succinate to complex II and complex I. **B)** Left: Complex I activity after incubating permeabilised turtle mitochondria with MitoSNO, MitoNAP (vehicle), or H<sub>2</sub>O (control) in the absence and presence of the thiol-reducing agent DTT (N=5). Right: Representative traces of complex I activity. Arrow denotes addition of the complex I inhibitor rotenone. **C)** and **D)** Representative traces of ROS production, oxygen concentration and respiration rate over time of heart mitochondria before and after addition of **C)** MitoSNO or **D)** water. Mitochondria were incubated with succinate and allowed to respire to anoxia. After 25 min of anoxia, MitoSNO, MitoNAP (vehicle) or water (control) was added (marked by the arrow), and after another 5 min of anoxia mitochondria were reoxygenated for ~2 min (marked by dotted line) by lifting the chamber stoppers. Respiration rate and ROS production were then recorded again, and rotenone (Rot) was added. Horizontal black bars indicate the time span for quantification of respiration rate and ROS production (at [O<sub>2</sub>] of 145 μmol l<sup>-1</sup> before and after anoxia and reoxygenation and at [O<sub>2</sub>] of 100 μmol l<sup>-1</sup> after addition of rotenone). Quantification of **E)** ROS production and **F)** respiration rate of mitochondria (N=5) before and after anoxia and reoxygenation (A/R) and with rotenone, incubated with MitoSNO, MitoNAP or water (control) during anoxia as shown in panel C) and D). Data are shown as means ± SEM. Asterisks denote a significant difference between groups (P<0.05).

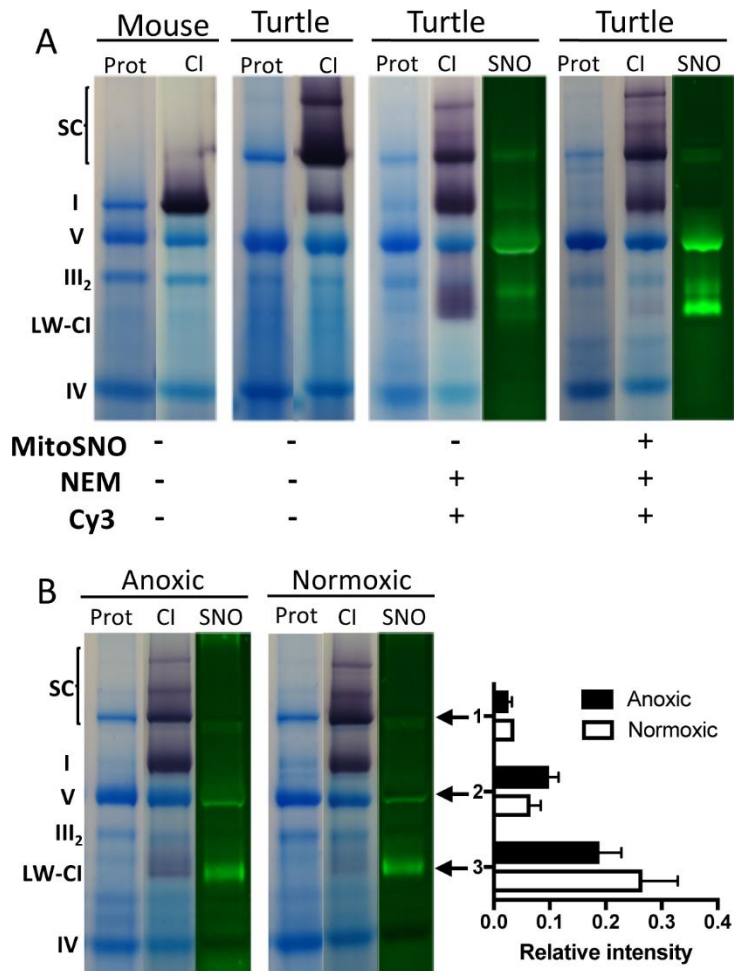


**Figure 4.** Heart mitochondrial complexes and S-nitrosation. **A)** BN-PAGE of mitochondrial protein complexes (Prot, blue), complex I NADH-reductase activity (CI, purple) and S-nitrosation (SNO, green) of heart mitochondrial complexes treated with MitoSNO, NEM and Cy3 as indicated, isolated from mouse and warm normoxic turtles. Mouse heart mitochondria were included to identify mitochondrial complexes (I, V, III<sub>2</sub> (dimer), IV; left). SC indicates supercomplex and LW-CI the flavin-containing matrix-arm of complex I with NADH-reductase activity. **B)** S-nitrosated mitochondrial complexes in heart mitochondria from turtles acclimated to 5°C and exposed to anoxia (N=5) or normoxia (N=5) (left panel), and their relative intensity (right panel) shown as means ± SEM (N=5). The intensity of the Cy3 fluorescence (green) was quantified relative to the protein stain of complex V, as explained in Materials and Methods. 1: Supercomplex, 2: Complex V, 3: LW-CI. There was no significant difference between anoxic and normoxic values (P>0.05).

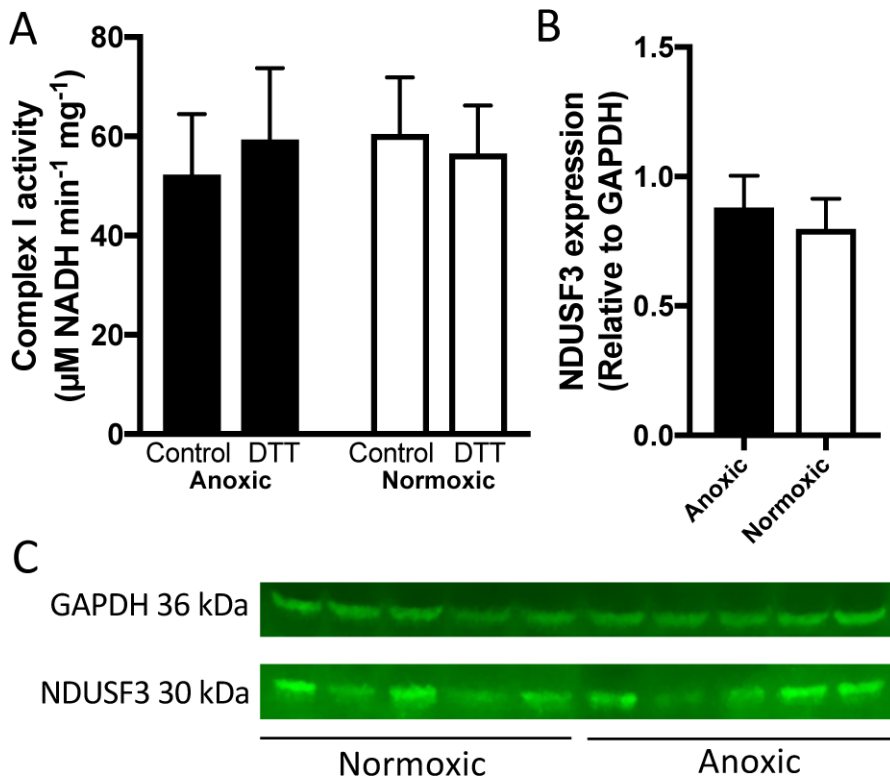


**Figure 5.** Complex I activity in heart mitochondria from turtles acclimated to 5° C and exposed to anoxia (N=5) or normoxia (N=5). **A)** Complex I activity of mitochondria incubated with the thiol reducing agent DTT or without (control). **B)** Quantification of complex I expression (NDUSF3 subunit) relative to GAPDH by western blotting **C)** Western blot of complex I (NDUSF3) expression with GAPDH as loading control in heart tissue samples from normoxic and anoxic turtles. Data are shown as means  $\pm$  SEM. There was no significant difference between groups ( $P > 0.05$ ).